(Preprint) AAS 18-249

SMALLSAT NAVIGATION VIA THE DEEP SPACE NETWORK: INNER SOLAR SYSTEM MISSIONS

Jeffrey R. Stuart* **and Lincoln J. Wood†**

The space industry has seen an explosion in the number of operational SmallSats in Earth orbit, with a natural interest in extending SmallSat capabilities outside of low Earth orbit. As with larger missions, near-term deep-space SmallSats will rely on the Deep Space Network or similar facilities. Given the predicted growth in the number of deep space missions, effective use of DSN resources will be more critical than ever. Our investigation provides an initial survey of expected inner Solar System navigation performance for DSN radiometric data types, from two-way Doppler and ranging to one-way equivalents, including delta differential one-way range and alternative tracking strategies.

INTRODUCTION

The cost of launch into orbit presents one of the greatest barriers to access to space, with large launch vehicles required for even relatively modest payload masses. On the other hand, the miniaturization of spacecraft components, and the CubeSat form factor in particular,[1] has lead to a renewed interest in smaller, more agile missions within the space community. Couple this interest with the proliferation of rideshare opportunities easing access to orbit for smaller payloads and it's no wonder that we have seen an explosion in the number of operational SmallSats in Earth orbit. Naturally, the interest in SmallSat capabilities extends outside of LEO, with JPL currently flying MarCO[2] toward Mars as well as planning to send INSPIRE,[3] Lunar Flashlight,[4] and NEAScout[5] beyond Earth orbit. Future deep-space SmallSats will more than likely rely on the telecommunications and tracking capability of the Deep Space Network (DSN) or similar entities, as the MarCO spacecraft are doing. Given the predicted growth in the number of deep space missions, we expect that DSN resources will be in high demand, even with the capability to support Multiple Spacecraft Per Aperture (MSPA).

As a general rule, SmallSat missions are cost effective because rideshare opportunities are cheaper than dedicated launches; and a common form factor encourages the development and compatibility of off-the-shelf components. A common misconception, however, is that these cost savings necessarily extend to all aspects of the mission, including operations and telecommunications. For example, costs for mission design and navigation are directly tied to the complexity of the mission as well as the attendant navigation requirements and are nearly insensitive to the actual size of the spacecraft. In fact, it is entirely conceivable that a SmallSat mission could levy more stringent position or velocity knowledge requirements than a mission with a larger spacecraft. Accordingly, any

*Research Technologist, Mission Design and Navigation Section, Jet Propulsion Laboratory, California Institute of Technology, jeffrey.r.stuart@jpl.nasa.gov

†Principal Engineer, Mission Design and Navigation Section, Jet Propulsion Laboratory, California Institute of Technology, lincoln.j.wood@jpl.nasa.gov

savings in operational cost, effort, or DSN use will more than likely arise from careful assessment of the mission class, the relevant risk posture, and any associated impacts on or relaxation of operational requirements. While all missions will eventually develop their own detailed navigation plans, a common set of references is needed to support SmallSat missions, especially in the early development phases.

While there is an extensive literature on the subject of deep-space navigation, most works focus on analyzing specific mission concepts and are not broad surveys of navigation capability. Lincoln Wood has authored a series of papers detailing the historical development of deep space navigation, covering trends and specific missions up to 2009.[6–10] Even these literature surveys, however, don't present DSN tracking options in a convenient format for perusal and selection by future missions. A previous investigation addressed this need for a high-level view of the navigation performance that cislunar SmallSat missions can expect when using the DSN.[11] In this investigation, we extend the analysis to interplanetary missions within the inner solar system while covering a broad range of tracking scenarios utilizing multiple different measurement types:

1. two-way Doppler and ranging measurements using X- and Ka-bands;
2. equivalent one-way measurements enabled by precise on-board clocks;
3. Delta Differential One-way Ranging (DDOR); and,
4. alternative strategies wherein longer passes are split into shorter segments.

The performances of one-way tracking and pass sub-sampling techniques are of particular interest because these strategies can exploit MSPA; multiple spacecraft can downlink to the ground station while one satellite is receiving uplink. Our goal is to provide a catalogue of options for DSN support, with reasonable performance estimates, which prospective SmallSat missions can use to predict required staffing and funding levels for their own development and operational needs. The following sections detail our analysis approach as well as qualitative discussions of the results for various tracking scenarios; the appendix contains comprehensive tabulations of the results.

NAVIGATION SIMULATION APPROACH

To characterize navigation performance, we investigate state reconstruction and prediction accuracy using straightforward covariance analysis; a detailed mathematical description of this analysis technique can be found in Chapter 6 of *Statistical Orbit Determination*.[12] We focus on characterizing the performance associated with traditional measurements from the DSN ground stations at Goldstone, Madrid, and Canberra, although our results should be broadly applicable to similar international and domestic partner sites. We performed all trajectory and navigation simulations using JPL's Mission Analysis, Operations, and Navigation Toolkit Environment (MONTE);[13] planetary ephemerides are provided by JPL's HORIZONS database.[14]

Traditional Two-Way Radiometric Data Types

Two-way Doppler range-rate is the most commonly used data type supplied by the DSN. Two-way Doppler measurements originate as a signal transmitted by one of the DSN ground stations; spacecraft receive this signal then relay it back to the transmitting antenna on Earth. Measured differences in frequency between the transmitted and the received signals are subsequently translated to spacecraft line-of-sight velocity estimates. Given sufficiently long tracking passes, two-way

Doppler measurements provide a wealth of information about the spacecraft orbital motion as well as the surrounding dynamical regime.[15] Indeed, such tracking information is the primary data type for host of planetary gravity science investigations. Similarly, two-way ranging is available through the DSN via the Sequential Ranging Assembly (SRA), which converts two-way light times into range units. Throughout this investigation we will use the acronym SRA to refer primarily to the two-way ranging data provided by the ranging assembly, though technically SRA refers to the hardware system. However, two-way measurements necessarily require dedicated support from a DSN antenna for the duration of a tracking pass, limiting their availability as the number of spacecraft in operation grows larger. Furthermore, SmallSat missions might be considered of lower priority than larger missions, meaning that already sparse tracking schedules may be disrupted if a higher priority mission needs to recover from a safe mode or other upset event. Thus, we also consider the use of alternative data sources, specifically one-way Doppler, one-way Range and Differential One-Way Range (DDOR). Brief descriptions of these data types are presented in the following sections; more rigorous mathematical treatments of the data types can be found in Moyer,[16] with DSN-specific data provided by the DSN Link Design Handbook.[17] For the majority of this investigation, uplink and downlink are both assumed to be X-band, regardless of the specific measurement type used; analysis which uses Ka-band will be explicitly noted as such. The data weights used for our analysis are presented in Table 1. X-band two-way and DDOR noises are standard values used for a variety of deep space missions, while Ka-band weights are representative of those used for a flight demonstration on the Juno spacecraft.

Table 1. Data weights used for covariance simulation, all noises 1-σ.

Parameter	Value	Units
X-band frequency	7.9×10^{9}	Hz
Ka-band frequency	32.0×10^{9}	Hz
Two-way Doppler noise (X)	5.62×10^{-3}	Hz
Two-way Doppler noise (Ka)	2.15×10^{-2}	Hz
Two-way SRA noise (X)	1.0	m
One-way Doppler noise (X)	8.17×10^{-2}	Hz
One-way range noise (X)	5.0	m
CSAC white noise (1-day)	2.15×10^{-3}	Hz
CSAC random walk (1-day)	6.44×10^{-2}	Hz
CSAC Allan deviation (1-day)	4×10^{-11}	s/s
DDOR noise (X)	0.06	ns

Modeling of One-Way Radiometric Tracking

Opportunistic use of one-way Doppler tracking via the DSN's MSPA capability may provide an alternative data source for state estimation, one that can take advantage of a tracking pass whose primary target is another spacecraft or when multiple spacecraft are sharing one tracking pass. In contrast to two-way measurements, we model one-way measurements as originating on the spacecraft and being received by ground stations; for antennas that can receive and record multiple signals, tracking data for multiple spacecraft can be simultaneously captured. Note that one-way ground-to-spacecraft signals are also possible, but present slightly different operational paradigms. Our analysis considers two- and one-way tracking as entirely separate cases; however, there is no reason

that these distinct types of tracking passes cannot be alternated throughout the course of a mission. The following discussion details some of the steps taken to model one-way Doppler and ranging tracking in our investigation.

One primary reason that one-way tracking is uncommon for deep-space applications is the need for precise timing information provided by an extremely accurate and stable on-board clock. Thus, two-way tracking has traditionally been favored due to the increased accuracy of ground-based atomic clocks and the relative availability of dedicated DSN tracking intervals. However, as the number of spacecraft operating across the solar system grows, there is additional pressure to be more efficient in the use of the DSN's limited resources. In turn, this has prompted the development of space-based atomic clocks appropriate for deep-space applications; the aptly named Deep Space Atomic Clock (DSAC) will soon be available for larger spacecraft[18] while Chip-Scale Atomic Clocks (CSACs) are currently being considered for SmallSats.[19] Ultra-stable oscillators (USOs) can provide the needed accuracy over intervals of 100s of seconds,[20] though gaps in tracking fail to capture random walks in the USO, leading to degraded navigation solutions.

Since two-way tracking has dominated deep-space navigation for the past several decades, comparatively little navigation software development has focused on supporting one-way measurement types. Indeed, only recently has MONTE begun to infuse precise on-board clock models and link them to the appropriate one-way measurement types so that accurate filtering simulations can be performed. Because of this relatively recent development history for the clock models, we have instead favored use of the more historical, and validated, spacecraft frequency models. While these frequency drift models may not be as precise as direct clock models, they are sufficiently accurate to support the covariance analyses presented in this investigation; we leave it as future work to fully validate the covariance assessments with more rigorous filtering simulations. For our analysis, we have transformed the performance specifications of the SA.45S Chip Scale Atomic Clock[19] into appropriate values for frequency stability, as shown in Table 1.

Delta Differential One-Way Range Measurements

Delta Differential One-Way Ranging (DDOR) is commonly used to obtain precise plane-of-sky angular measurements to complement line-of-sight Doppler and range data. A spacecraft typically transmits special DOR tones which are received by two ground station antennas separated by a large geographic distance; for the analysis cases presented here, we alternate DDOR passes between Goldstone-Madrid and Goldstone-Canberra baselines. In fact, this alternation of baselines over a given tracking schedule is critical: if only one baseline is used, large state uncertainties can still remain in one axis lying in the plane-of-sky. Precise geometrical measurements of the spacecraft state are obtained by tracking the spacecraft range difference as measured by the two ground stations. Measurement errors due to atmospheric disturbances are eliminated by characterizing the atmospheric effects on a known quasar source. Because the measurement is the range difference observed by the two ground stations, on-board clock errors are differenced out, enabling precise measurements regardless of spacecraft frequency stability. In addition to the extra information from the alternative data type, one advantage to using DDOR is short tracking durations of 30-min to 1-hour; on the other hand, two antennas must be used, and DDOR passes can only occur where there are overlaps in coverage. Thus, the availability of DDOR is heavily dependent on DSN usage and the orbital geometry of the spacecraft in question. While we only consider the DSN-specific baselines, partner sites supported by ESA, JAXA, and ISRO can also be used to form DDOR baselines with DSN stations, enabling some additional freedom in scheduling at the cost of potential

(a) 8-hour pass decimated to 2 or 3 30-min. passes

(b) 4-hour pass decimated to 2 30-min. passes

Figure 1. Schema showing pass sub-sampling strategy.

degradations in measurement accuracy.

Pass Sub-Sampling

When multiple spacecraft are within the same beam width of a DSN antenna, they are able (and may be required) to operationally cycle between being the primary contact with the DSN. This cycling then enforces a sub-sampling behavior on each spacecraft wherein a longer monolithic pass is decimated into a series of shorter passes as illustrated in Fig. 1. When a spacecraft is the main contact with the DSN, it is assumed to be capable of two-way tracking; other spacecraft may take advantage of one-way tracking provided they have the required clock stability. While individual short passes may provide little in the way of orbit determination information, multiple passes within a short sequence may provide dynamical information approximating the information content of longer passes, as described by Hamilton and Melbourne.[15] We therefore assess these tracking scenarios, sub-sampling 8-hour and 4-hour passes as shown in Fig. 1; the 4-hour scheme could also represent a case where an 8-hour pass is sampled over only two intervals (e.g., at beginning and middle or at middle and end). For this initial analysis we assume that tracking occurs only during the two-way contact intervals; we leave the inclusion of one-way tracking for future analysis.

Reference Spacecraft Trajectory

Our current use case focuses on state reconstruction and prediction for spacecraft within the inner solar system but far from any major gravitating bodies. Specifically, we seek to characterize the performance of an Earth-trailing trajectory residing in the ecliptic plane, as illustrated in Fig. 2. We focus our efforts on the highlighted region at approximately 0.7 AU from Earth. Although our sample path has no particular end destination, a number of mission concepts provide similar dynamical environments and observational constraints, for example:

- sentinel / observer missions to the Sun-Earth Lagrangian points, particularly L_4 and L_5;
- asteroid flyby or rendezvous missions; and,
- interplanetary cruise, for example Earth-Mars or Earth-Venus.

While these differing cases may involve dissimilar state knowledge requirements or prediction horizons, they are united by their relatively benign environment in terms of gravitational dynamics. That is, the gravity of the sun plays a dominant role in the heliocentric path of the spacecraft while other planetary bodies provide at most slight perturbations to the motion. All bodies are modeled as point masses for this simulation case. Other perturbing effects may include solar radiation pressure (SRP) and unbalanced attitude control maneuvers; for our scenario, we assume a stochastic acceleration

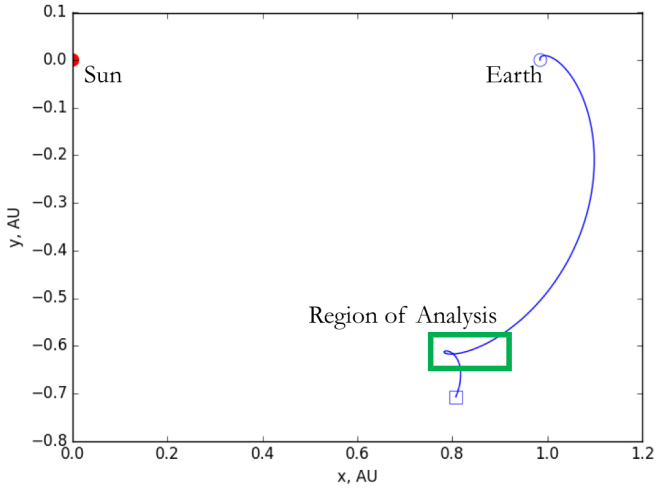

Figure 2. Earth-trailing trajectory, shown in Sun-Earth rotating frame.

of $1.1 \times 10^{-12}\ km/sec^2$ in daily batches due to uncertainties in SRP (comparable to the value from the MRO cruise phase[21]) and weekly momentum desaturation maneuvers.

For this particular mission scenario, the long interplanetary distances may entail high-gain antennas to communicate with ground stations on Earth, where these antennas usually have directed gain patterns. But, due to the large variations in Sun-Probe-Earth angles, special consideration must be made for pointing a directed communication antenna. On sufficiently large spacecraft, this can be accomplished by gimbaling the antennas or the solar arrays such that communication and sun-pointing of the arrays can be maintained simultaneously. However, this option may not be available for smaller spacecraft with tighter mass and volume constraints; indeed, even for larger spacecraft such mechanical solutions may be undesirable for a variety of reasons. Regardless, many SmallSat designs entail fixed geometry for the solar arrays and high-gain antennas, requiring that the spacecraft point away from the optimal electrical power generation attitude in order to communicate with Earth. This, in turn, can sometimes lead to very strict constraints on tracking duration and frequency. Even when low- or medium-gain antennas are viable options, these data-constrained alternatives may preclude collection of both Doppler and range measurements. Additionally, SmallSat constraints on battery sizing and thermal systems may further impact the length of time that the on-board transmitter can operate. When we combine this with the small budget of a typical SmallSat mission, the limited tracking resources of the DSN, and the fact that MSPA will only be useful when spacecraft are clustered together, we can expect that interplanetary tracking will be short and sparse, even in the inner solar system.

DOPPLER-ONLY TRACKING

This section presents a qualitative discussion of Doppler tracking performance in the inner solar system. Two-way, X-band tracking uncertainties provide a standardized baseline, while one-way tracking results indicate the performance available from MSPA and other one-way scenarios. Performance of Ka-band tracking is compared to X-band, and alternative strategies to selectively decimate longer passes are analyzed. Tabulated results for X-band two- and one-way tracking cases are contained in the appendix; comparative values for Ka-band and pass sub-sampling can be inferred

based upon the discussion below.

Two-Way Doppler Tracking

We begin by focusing on the expected navigation performance available using two-way Doppler measurements in the X-band, where these results serve as a useful baseline of comparison for other tracking scenarios. Furthermore, we can assess a minimal level of performance from DSN communications, as some amount of two-way communication is required for every mission. We run covariance analyses for a variety of weekly tracking schedules and tracking pass durations, namely:

- tracking 1, 2, 3, or 7 times a week; and,
- tracking pass durations of 30 minutes, 1, 2, 4, or 8 hours,

for a total set of 20 cases. Tables with summary results for state reconstruction and forward prediction specific to two-way Doppler tracking are contained in the appendix; here we reproduce one table (Table 2) to illustrate and inform our discussion. All covariance values presented in this analysis are 1-σ unless otherwise noted. For our purposes, "reconstruction" is defined to mean the ability

Table 2. Two-way Doppler-only position reconstruction accuracy at data cut-off. Approximate values of the principal axes of the uncertainty ellipsoid, in km.

Passes	**Pass Duration**				
Per Week	30 min.	1 hr.	2 hrs.	4 hrs.	8 hrs.
1	(406.8, 58.26, 31.48)	(237.49, 35.27, 30.85)	(138.26, 31.77, 19.99)	(46.57, 31.46, 9.87)	(31.73, 14.68, 3.24)
2	(251.17, 31.82, 18.92)	(94.79, 31.79, 18.52)	(42.6, 31.64, 16.26)	(31.15, 21.45, 6.81)	(28.85, 10.26, 2.06)
3	(196.26, 31.69, 16.66)	(79.94, 31.64, 16.29)	(36.88, 31.23, 14.23)	(30.58, 18.11, 5.54)	(26.55, 9.03, 1.77)
7	(105.59, 30.89, 12.42)	(55.39, 30.61, 10.88)	(30.46, 27.72, 8.02)	(28.79, 13.2, 3.24)	(21.34, 5.47, 1.25)

to bound the state up to the epoch of data cut-offs (DCOs) for the last tracking pass. For this case, "prediction" is the estimation of a state up to one month after DCO. As is expected, navigation performance improves with more frequent tracking and longer passes. However, securing longer continuous tracking passes, if they can be supported by the spacecraft, seems to be a more effective strategy than increasing the number of passes; note, for example, that one weekly pass of 8 hours is comparable in both reconstructive and predictive power to daily passes of 2 to 4 hours. Note also the apparent law of diminishing marginal utility (a phrase we freely borrow from economics): at some point increases in pass frequency and duration provide only modest improvements in uncertainty, at least in terms of absolute values.

Some notable aspects of the state uncertainty time history are not captured by the simple quantitative comparison presented so far. Thus, we turn to an assessment of the evolution of the covariance ellipsoids over time. Figure 3 illustrates the time history of the principal components of the 3-D position and velocity uncertainty ellipsoids for one pass per week; the a-, b-, and c-axes are the major, intermediate, and minor principal axes of the uncertainty ellipsoid, respectively. Note that for tracking durations of 1 hour or less, the major and intermediate axes of the position covariance grow from the initial epoch of the simulation, through DCO, and on to the end of the prediction interval. Likewise, velocity covariances are degraded for these cases as well. By implication, the estimates of other spacecraft parameters such as maneuver execution errors and solar radiation pressure (SRP) would be equally suspect. It is worth noting, though, that even relatively short two-way tracking passes may be sufficient for reconstructing the state and other spacecraft parameters for

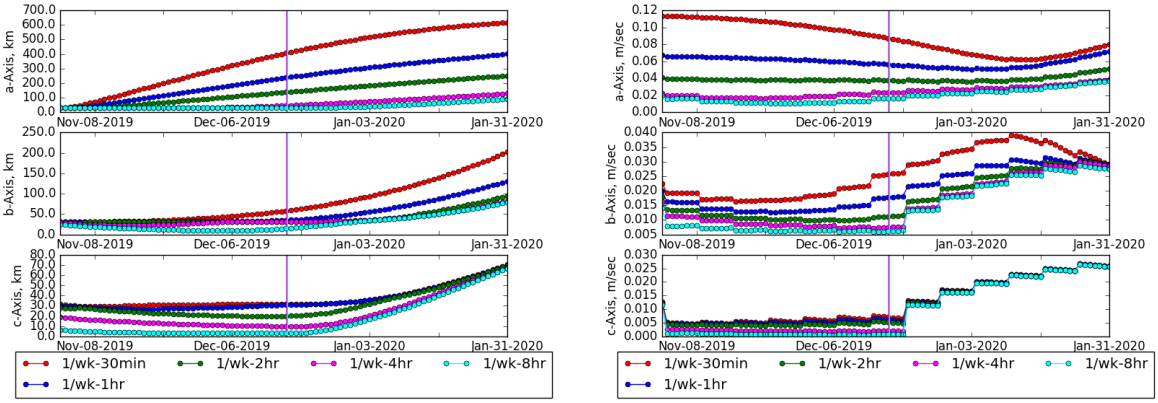

$(a) Position$ $(b) Velocity$

Figure 3. Growth in position and velocity uncertainty for 2-way Doppler only, 1 pass per week. Vertical lines are data cut-offs (DCOs).

many mission scenarios, and some negative effects of sub-hour tracking can be removed by the addition of one extra tracking pass per week. As we show in Fig. 4, increasing the number of tracking

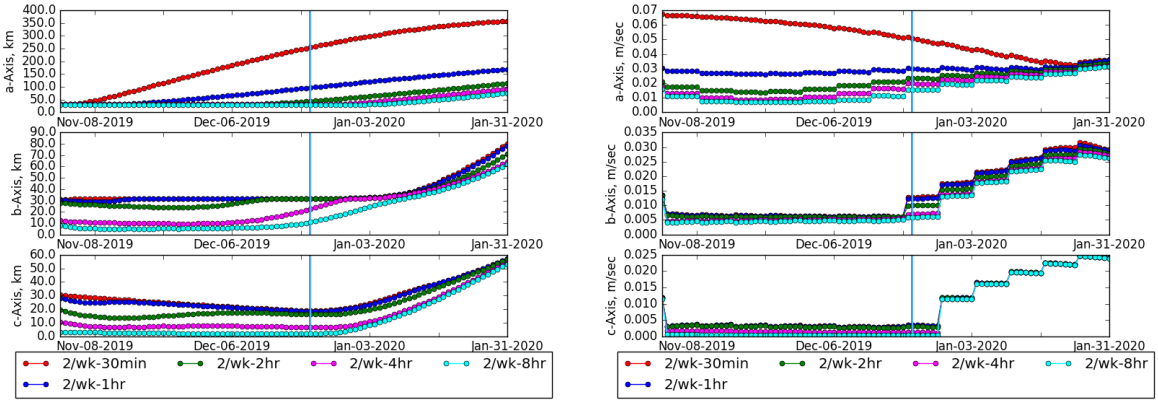

$(a) Position$ $(b) Velocity$

Figure 4. Growth in position and velocity uncertainty for 2-way Doppler only, 2 passes per week. Vertical lines are data cut-offs (DCOs).

passes removes pre-DCO kinks and spreads in the velocity reconstruction, indicating that additional components of the maneuver performance are resolved. In contrast, the qualitative behavior of the largest position principal axis does not change, even if tracking is increased to a daily occurrence. This observation reinforces two common rules of thumb in deep-space navigation:

1. Keep tracking passes sufficiently long in order to:
   (a) resolve stochastic or bias effects of long-term perturbations like SRP or gravity mismodeling; and
   (b) ascertain right ascension and declination information from the Earth's rotational signature (Hamilton-Melbourne Theory).[15]

2. Budget $n + 1$ tracking passes for every n maneuvers in order to characterize thruster performance, -or- perform maneuvers in the middle of longer tracking passes.

Figs. 3 and 4 highlight the behavior of the principal axes of the covariance ellipsoid; however, some comment should be made as to the relative direction of the largest uncertainties. For sparse, short tracking passes, the dominant uncertainty direction is out of the plane of the ecliptic. For longer or more dense tracking passes, this out-of-ecliptic uncertainty remains the largest component, but only by a moderate factor above the in-plane components of the uncertainty.

One-Way Doppler Tracking

We turn now to the one-way Doppler measurement type, where we begin our analysis by considering one-way Doppler measurements as the sole information source for state estimation (note our assumed use of a CSAC for precise timing). In reality, some two-way communication may be intermixed with the one-way passes; however, we neglect this consideration in favor of the more conservative one-way only scenario. As with two-way tracking, we run cases for 1, 2, 3, and 7 passes per week and 30-min, 1-, 2-, 4-, 8-hour durations. Overall, the same general trends emerge for one-way as for two-way tracking, though with maximum uncertainties roughly 5 times larger than for pure two-way tracking: longer durations are more beneficial than multiple passes and the marginal utility of additional tracking quickly drops off. However, the time-history behavior of the covariances shows remarkable degradation, as is evidenced by Fig. 5.

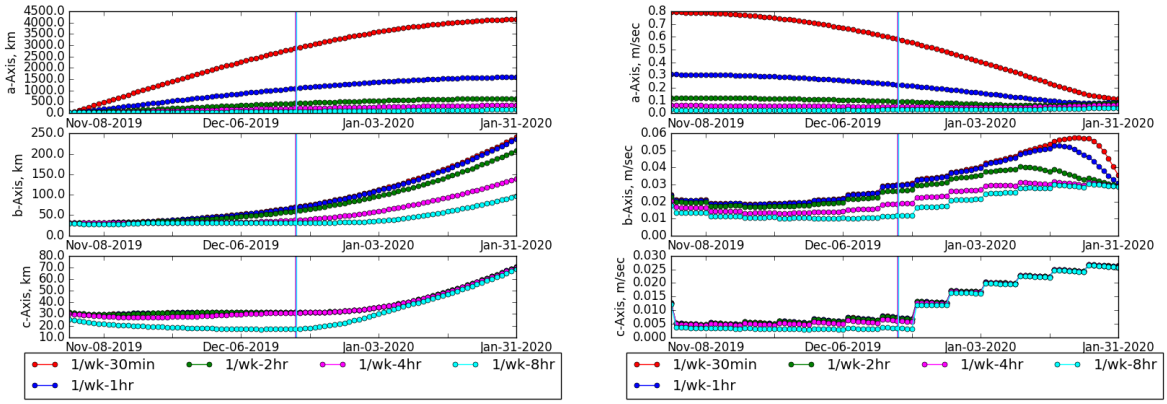

$(a) Position$ $(b) Velocity$

Figure 5. Growth in position and velocity uncertainty for 1-way Doppler only, 1 pass per week. Vertical lines are data cut-offs (DCOs).

Doppler Tracking via Ka-band

We next consider the use of an alternative radio band, Ka, for two-way Doppler tracking. Ka-band is likely to grow in usage for DSN supported missions because it supports higher data rates and greater signal-to-noise ratios (SNR). This improved performance is important for several use cases, including gravity science, which benefits from lower noise, as well as solar conjunction and other high SNR scenarios. However, for the scenarios investigated, Ka-band offers no great improvement over X-band tracking, as shown in Fig. 6. While improved noise performance is somewhat beneficial, considerations such as pass length, tracking frequency, and viewing geometry have larger

impacts. This last point is particularly important to note, since the DSN currently has only one station capable of Ka-band uplink; for the foreseeable future, two-way Ka tracking will be extremely limited, with dual X-uplink and Ka-downlink more regularly available. These covariance estimations have been anecdotally validated by experimental use of Ka-band tracking on Juno, which saw little to no improvement to orbit determination in the Jupiter system. However, relatively few spacecraft have even tested Ka-band tracking, let alone used it for actual operations; as experience develops with this new capability, expected performance and best practices will continue to evolve.

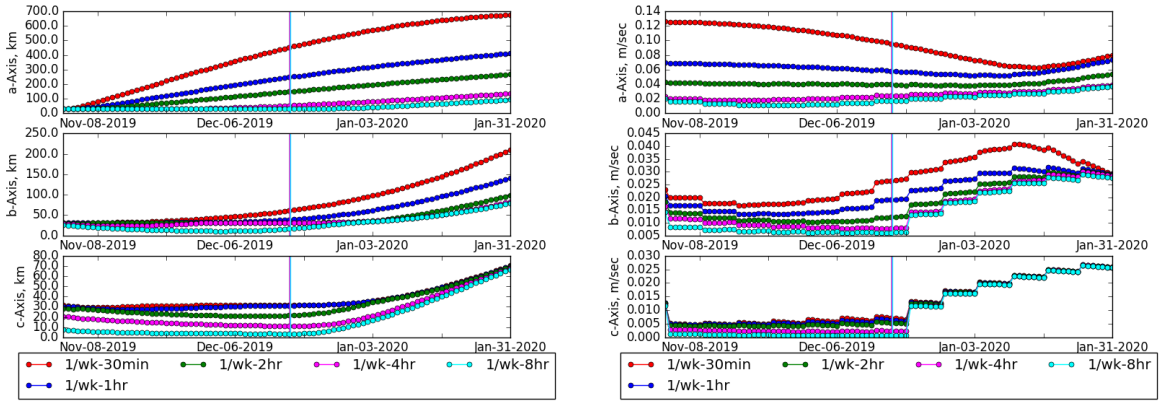

$(a) Position$ $(b) Velocity$

Figure 6. Growth in position and velocity uncertainty for 2-way Ka-band Doppler only, 1 pass per week. Vertical lines are data cut-offs (DCOs).

Sub-Sampling of Doppler Tracking

As the final permutation of Doppler-only tracking, we turn to the sub-sampling of longer tracking passes, where the goal is to reduce the total amount of time spent tracking a single spacecraft while still retaining the orbit determination performance of longer passes. We thus consider the decimation of weekly 4- and 8-hour tracking passes and compare these sparser data volumes to more traditional monolithic 1-, 4-, and 8-hour full passes, as displayed in Fig 7. As we can see, the sub-sampled passes offer clear improvements over short, 1-hour tracking passes; the one exception to this trend is the intermediate uncertainty axis for the case sampling only the beginning and end of the 4-hour pass. On the other hand, the decimated 8-hour strategy which retains the beginning, middle, and end performs nearly identically to the full 8-hour pass. These results indicate that a sub-sampling tracking strategy enabled by MSPA is a viable route to improved DSN usage without significant degradation in navigation performance. Thus, clusters of spacecraft may benefit from a form of "collective bargaining" wherein multiple smaller missions agree to split a longer DSN pass when negotiating DSN coverage, amortizing the fixed costs of the DSN usage. Some applications for when spacecraft are not within the same beam-width may be viable, but would have to account for the built-in set-up and tear-down times associated with current DSN operations. Note that one-way tracking is not included in the pass sub-sampling analysis, though in principle that data type would be available and could be used to further improve performance.

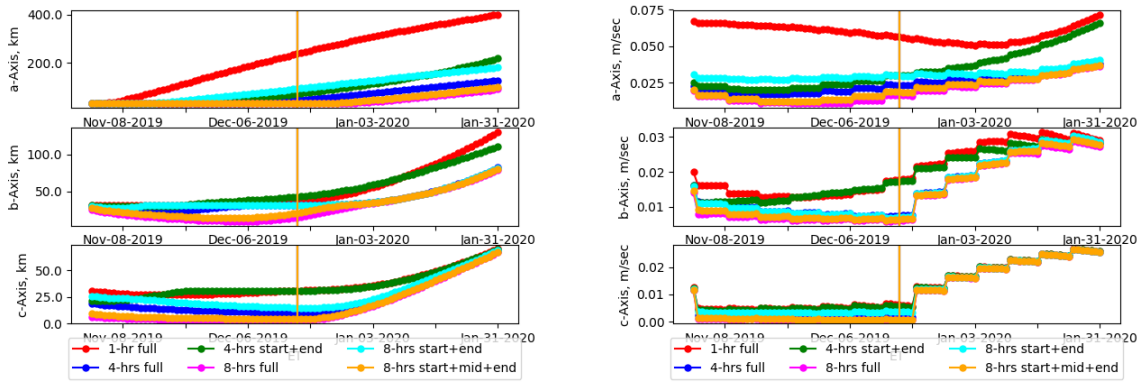

$(a) Position$ $(b) Velocity$

Figure 7. Growth in position and velocity uncertainty for 2-way Doppler only, 1 pass per week, different sub-sampling strategies. Vertical lines are data cut-offs (DCOs).

ADDITIONAL MEASUREMENT TYPES

We now consider the use of supplemental measurement types in conjunction with, or in place of, traditional Doppler measurements. In particular, we focus on ranging data types, either via single-antenna methods which provide additional line-of-sight information or through the use of DDOR which provides plane-of-sky knowledge.

Range Data Types

We first consider traditional ranging schemes which can be performed simultaneously with Doppler measurements. As can be seen for two-way SRA in Fig. 8, the performances in Doppler-only and ranging-only are similar in magnitude, if not exact qualitative behavior. However, when the measurements types are considered simultaneously, as in Fig. 9, the performance is significantly improved for tracking passes of 1 hour or less. On the other hand, two-way ranging has the potential to degrade telemetry, so its use cannot always be assumed for all cases. One-way ranging has a similar performance boosting capability when used in conjunction with one-way Doppler, though we remind the reader that the combined simulation results should be treated especially cautiously, given the previously mentioned modeling limitations.

Delta Differential One-way Range

We now consider the addition of DDOR data in the two- and one-way tracking scenarios discussed previously. Specifically, we include either monthly or weekly DDOR tracking passes interspersed within the already established Doppler schedules. The following discussion focuses on these two cases and their implications for deep-space navigation; for this analysis, DDOR tracking passes are assumed to be 30 minutes in duration.

The inclusion of monthly DDOR passes into sparse tracking schedules dramatically decreases state uncertainty, as can be seen when comparing the covariance values for two-way Doppler in Table 3 to those in Table 2. In particular, note that one DDOR pass per month combined with once-per-week, 30-min, two-Way Doppler passes produces reconstructed and predicted uncertainties comparable to daily passes of 30-min duration or weekly passes of 1-4 hours. The effects are

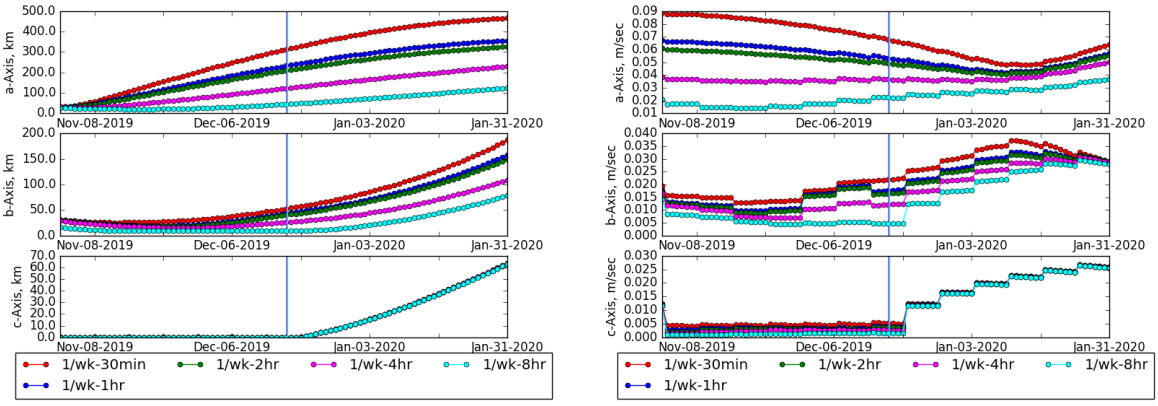

$(a) Position$ $(b) Velocity$

Figure 8. Growth in position and velocity uncertainty for 2-way SRA, 1 pass per week. Vertical lines are data cut-offs (DCOs).

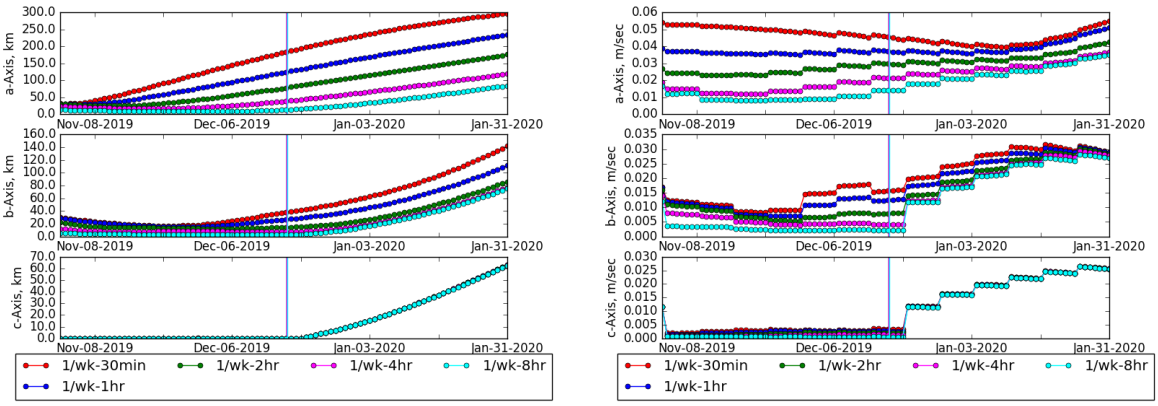

$(a) Position$ $(b) Velocity$

Figure 9. Growth in position and velocity uncertainty for 2-way Doppler plus SRA, 1 pass per week. Vertical lines are data cut-offs (DCOs).

even more dramatic when DDOR is used in conjunction with one-way Doppler tracking, where this combination produces navigation uncertainties below that of purely two-way tracking without DDOR.

Table 3. Two-way Doppler plus monthly DDOR position reconstruction accuracy at data cut-off. Approximate values of the principal axes of the uncertainty ellipsoid, in km.

Passes Per Week	Pass Duration				
	30 min.	1 hr.	2 hrs.	4 hrs.	8 hrs.
1	(78.51, 31.45, 14.75)	(53.96, 31.27, 11.94)	(39.77, 30.79, 6.48)	(33.38, 27.96, 3.41)	(30.65, 12.79, 2.24)
2	(41.36, 30.39, 2.94)	(39.26, 30.16, 2.9)	(33.04, 27.51, 2.65)	(29.57, 18.83, 2.13)	(25.3, 10.26, 1.57)
3	(41.0, 29.64, 2.86)	(38.11, 29.29, 2.8)	(31.58, 25.49, 2.48)	(27.57, 16.26, 1.93)	(22.35, 8.75, 1.42)
7	(40.31, 28.46, 2.88)	(35.67, 27.68, 2.73)	(29.46, 22.34, 2.25)	(23.81, 13.18, 1.59)	(16.94, 5.71, 1.1)

An examination of the covariance time histories reveals an equally impressive change in qualitative behavior when DDOR tracking is included every month. Figures 10 and 11 illustrate the growth in uncertainty for two- and one-way Doppler tracking in conjunction with monthly DDOR. In both cases, the growth in uncertainty of the reconstructed states is delayed by the inclusion of monthly DDOR measurements. However, the growth prior to DCO is not entirely eliminated for short tracking passes; passes of at least two hours are required for consistent state reconstruction using two-way Doppler. Note also the "pinching" in the covariances at the epochs of the DDOR passes; the most accurate reconstructions will understandably be for epochs when the most precise measurements are available.

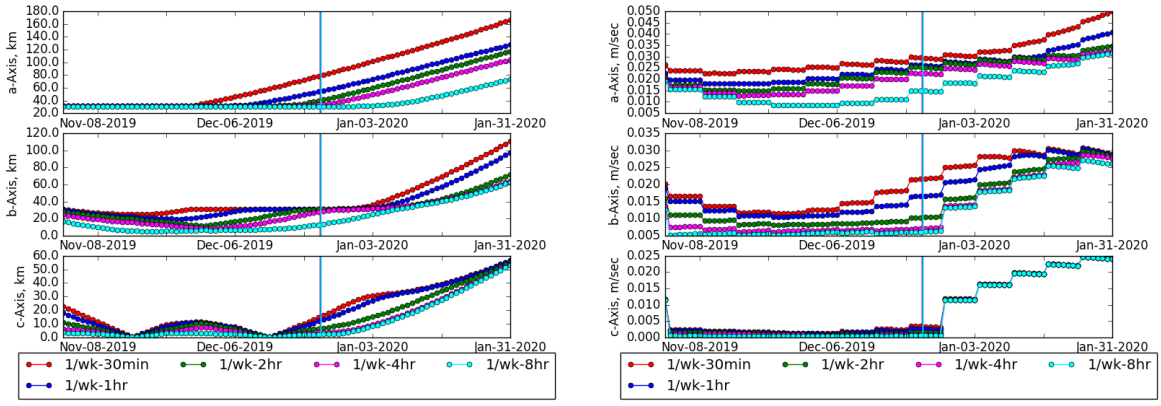

$(a) Position$ $(b) Velocity$

Figure 10. Growth in position and velocity uncertainty for 2-way Doppler plus DDOR: 1 Doppler pass per week, 1 DDOR pass per month. Vertical lines are data cut-offs (DCOs).

Weekly DDOR tracking further decreases state covariances, enabling even sparse and short two-way tracking to provide consistent state reconstructions. In contrast, even weekly DDOR tracking is not sufficient to provide consistent reconstructions for one-way tracking, regardless of pass duration or length; however, the associated uncertainty bounds are reduced.

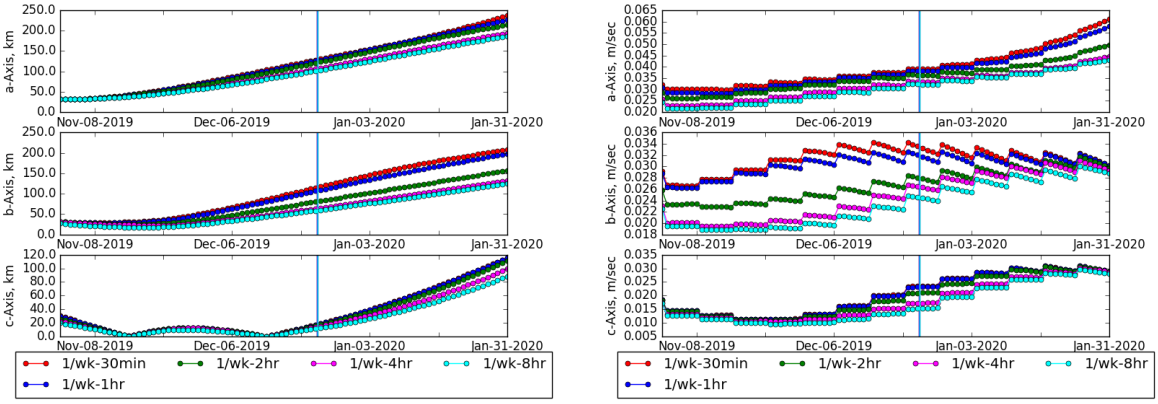

$(a) Position$ $(b) Velocity$

Figure 11. Growth in position and velocity uncertainty for 1-way Doppler plus DDOR: 1 Doppler pass per week, 1 DDOR pass per month. Vertical lines are data cut-offs (DCOs).

RESULTS IN BRIEF

We now briefly summarize the overall trends in the uncertainty covariance for the various cases considered. While detailed results are tabulated in the appendix, we wish to develop general rules of thumb to bound the expected changes in performance for different tracking strategies. To this end, Table 4 presents scaling values for both reconstruction and uncertainty using 2-way Doppler-only tracking as a reference covariance estimate; scaling is presented for both sparse (short and infrequent passes) as well as dense (long and frequent passes) tracking schemes. To interpret the table, treat the percentages as fractions of the 100% values from the 2-way Doppler case; that is, adding two-way SRA reduces the uncertainty RMS by roughly a factor of 2 for sparse schedules. On the other hand, reconstructed uncertainties associated with dense schedules can be decreased by an order of magnitude while prediction uncertainties are hardly changed by the addition of ranging data.

The most dramatic variations in Table 4 can be seen with sparse schedules and one-way data types; as we would expect, additional data has the most impact when information about the spacecraft trajectory is limited to begin with. We also observe that two-way tracking always outperforms equivalent one-way scenarios, but some combinations (e.g., 1-way Doppler and range) reduce uncertainties compared to purely 2-way Doppler tracking. There also appears to be a fundamental limit to forward prediction knowledge, regardless of the level of reconstruction ability; however, this is not terribly surprising given the inclusion of small stochastic effects such as acceleration uncertainty and desaturation maneuvers.

CONCLUSIONS

Efficient use of the tracking and telecommunications capability of the Deep Space Network is an increasing concern, especially given the predicted growth in the number of deep space missions. In particular, SmallSat missions with constrained budgets will need to be parsimonious in DSN usage and will need to carefully calibrate mission objectives and requirements to match available DSN support. As demonstrated throughout this investigation, precise state estimation relies on plentiful

Table 4. Approximate uncertainty scaling from 2-way Doppler-only baseline.

Analysis Case	Reconstruction	Prediction
2-way Doppler	100% (sparse)	100% (sparse)
	100% (dense)	100% (dense)
+ Range	50% (sparse)	50% (sparse)
	10% (dense)	100% (dense)
+ DDOR (monthly)	25% (sparse)	25% (sparse)
	100% (dense)	100% (dense)
1-way Doppler	700% (sparse)	700% (sparse)
	200% (dense)	125% (dense)
+ Range	75% (sparse)	75% (sparse)
	25% (dense)	100% (dense)
+ DDOR (monthly)	50% (sparse)	50% (sparse)
	300% (dense)	200% (dense)

and accurate measurement data, whether that information is from traditional two-way tracking or alternative data sources. Note that we have not considered relative navigation, whether for formations of spacecraft or for exploration of primitive bodies; inter-spacecraft ranging, optical navigation, or differential measurements may be required for applications where precise knowledge of relative states is required. However, we present a catalogue of DSN tracking scenarios for mission architectures within the inner solar system that planners can use to inform their initial trade studies. Qualitative results are summarized as follows:

1. Long duration Doppler passes enable precise navigation:
   (a) Two-way Doppler tracking, the most commonly used DSN measurement type, provides the baseline for comparison;
   (b) One-way Doppler measurements exploit the multiple spacecraft tracking capability of the DSN, but rely on precise clocks; even so, accuracy is generally an order of magnitude worse than two-way tracking;
   (c) Sparse tracking with short passes can meet loose positioning requirements, but with degraded capability to reconstruct the spacecraft state and other operational parameters;
   (d) Ka-band tracking offers no marked improvement over X-band; however, certain high signal-to-noise applications (e.g., tracking further into solar conjunction) may be enabled
   (e) Sub-sampling of longer tracking passes, perhaps coordinated among several spacecraft within an MSPA scenario, can offer performance nearly equivalent to (or at least not much degraded from) full tracking passes.
2. Ranging measurements, including DDOR, provide a complementary capability that:
   (a) Greatly improves navigation accuracies, though the effect is most pronounced for short and sparse Doppler passes;

(b) Enables reconstruction of additional spacecraft parameters when short Doppler passes are used;

(c) For DDOR, requires the use of two DSN antennas, though less frequently and for shorter intervals than Doppler measurements.

Tabulated results for different tracking schedules and mission architectures can be found in the appendix and are provided as a reference for mission planners. Note that these are just guidelines; selection of the proper schedule and measurement types will be mission dependent, especially since hardware limitations may necessitate short tracking passes. However, a variety of tracking options can provide comparable navigational accuracies, such that most missions should be able to find an option that satisfies their specific needs while still enabling efficient use of limited DSN resources.

In general, we expect state reconstructions based on Doppler data to be somewhat less effective when far from gravitating bodies, even if forward predictions may become more reliable. Briefly, Doppler provides a direct measurement of relative velocity and, therefore, we gain more insight into the current motion of the spacecraft when velocity changes are more pronounced. For interplanetary cruise applications, reconstructed position uncertainties can range from 1000s of km for the most sparse one-way tracking scenarios, to approximately kilometer-level accuracies for extensive two-way tracking. Likewise, forward prediction accuracies range from over 4000 km down to 10s of kilometers. Note that sparse one-way tracking schemes do raise concerns about acquiring contact with the DSN when close to the Earth: the 1-σ uncertainties in position are of the same order of magnitude as the X-band beam width of the 34-m antennas. However, opportunities for MSPA are expected to be relatively frequent if spacecraft are maintained in rough clusters, which in turn indicates that smallsat missions could rely in large part on one-way measurements as a major component of their navigation plan. Inclusion of ranging and/or DDOR has notable positive effects on navigation estimates; but, the best use of DDOR may remain to provide supplementary tracking for already sparse schedules to support close approaches to specific bodies, for example on asteroid flyby trajectories (though asteroid ephemeris errors will still be a significant factor). Although we focused on an Earth-trailing trajectory, our investigation could inform tracking analysis for other cruise scenarios within the inner solar system.

While this investigation comprehensively analyzed the navigation performance of Doppler and DDOR measurement types in straightforward tracking schedules, some avenues for future work remain. First, sample cases showing the effects of intermixing two- and one-way measurements would provide more realistic uncertainties for some possible operational paradigms, particularly the sub-sampling strategy. Second, accurate modeling of clock behavior and performance will increase the fidelity of one-way measurement simulations, providing a more accurate assessment of potential navigation performance. Finally, further analysis of Ka-band tracking is warranted, given the relatively few examples of this capability used in flight; in particular, future missions with Ka-band capability should be used to demonstrate and test the capability even if Ka is not the primary navigational data source.

ACKNOWLEDGEMENTS

This research was carried out at the Jet Propulsion Laboratory, California Institute of Technology, under a contract with the National Aeronautics and Space Administration.

REFERENCES

[1] California Polytechnic State University, *CubeSat Design Specification*, 13 ed., February 20, 2014. Accessed at: http://www.cubesat.org/resources/.

[2] S. Asmar and S. Matousek, "Mars Cube One (MarCO) - The First Planetary CubeSat Mission," *Mars CubeSate / NanoSat Workshop*, Pasadena, California, November 20–21, 2014.

[3] A. Klesh, J. Baker, J. Castillo-Rogez, L. Halatek, N. Murphy, C. Raymond, B. Sherwood, J. Bellardo, J. Cutler, and G. Lightsey, "INSPIRE: Interplanetary NanoSpacecraft Pathfinder In Relevant Environment," *Proceedings of the 27th Annual AIAA/USU Conference on Small Satellites*, Logan, Utah, August, 2013. SSC13-XI-8.

[4] P. Hayne, B. Cohen, B. Greenhagen, D. Paige, J. Camacho, R. Sellar, and J. Reiter, "Lunar Flashlight: Illuminating the Moon's South Pole," *Proceedings of the 47th Lunar and Planetary Science Conference*, Houston, Texas, March 22–25, 2016.

[5] J. Castillo-Rogez, L. Johnson, P. Abell, J. Bleacher, J. Boland, B. Farrell, L. Graham, and D. Thompson, "Near Earth Asteroid Scout Mission," *11th Meeting of the NASA Small Bodies Assessment Group (SBAG)*, Washington, DC, July 29–31, 2014.

[6] L. J. Wood, "The Evolution of Deep Space Navigation: 1962-1989," *Advances in the Astronautical Sciences: Guidance and Control 2008*, Vol. 131, 2008, pp. 285–308.

[7] L. J. Wood, "The Evolution of Deep Space Navigation: 1989-1999," *Advances in the Astronautical Sciences: The F. Landis Markley Astronautics Symposium*, Vol. 132, 2008, pp. 877–898.

[8] L. J. Wood, "The Evolution of Deep Space Navigation: 1999-2004," *Advances in the Astronautical Sciences: AAS/AIAA Spaceflight Mechanics Meeting 2014*, Vol. 152, 2014, pp. 827–847.

[9] L. J. Wood, "The Evolution of Deep Space Navigation: 2004-2006," *Advances in the Astronautical Sciences: AAS/AIAA Spaceflight Mechanics Meeting 2017*, Vol. 160, 2017, pp. 3271–3292.

[10] L. J. Wood, "The Evolution of Deep Space Navigation: 2006-2009," *2018 AAS/AIAA Spaceflight Mechanics Meeting*, Snowbird, Utah, August 20-23, 2018. AAS 18-226.

[11] J. R. Stuart and L. J. Wood, "SmallSat Navigation via the Deep Space Network: Lunar Transport," *IAF 68th International Astronautical Congress*, Adelaide, Australia, September 25-29, 2017. IAC-17-B4,3,12,x41638.

[12] B. D. Tapley, B. E. Schutz, and G. H. Born, *Statistical Orbit Determination*. Burlington, Massachusetts: Elsevier, Inc., first ed., 2004.

[13] S. Evans, W. Taber, T. Drain, J. Smith, H.-C. Wu, M. Guevara, R. Sunseri, and J. Evans, "MONTE: The Next Generation of Mission Design & Navigation Software," *The* 6^{th} *International Conference on Astrodynamics Tools and Techniques (ICATT)*, Darmstadt, Germany, March 14–17, 2016. https://indico.esa.int/indico/event/111/session/30/contribution/177.

[14] Solar System Dynamics Group, *HORIZONS System*. Jet Propulsion Laboratory, 2016. http://ssd.jpl.nasa.gov/?horizons.

[15] T. Hamilton and W. Melbourne, "Information Content of a Single Pass of Doppler Data from a Distant Spacecraft," Tech. Rep. JPL-SPS 37-39, Jet Propulsion Laboratory, California Institute of Technology, May 31, 1966. Accessed at http://descanso.jpl.nasa.gov/history/DSNTechRefs.html.

[16] T. D. Moyer, *Formulation for Observed and Computed Values of Deep Space Network Data Types for Navigation*. Hoboken, New Jersey: John-Wiley & Sons, Inc., 2003.

[17] Deep Space Network Project Office, *DSN Telecommunications Link Design Handbook*. Jet Propulsion Laboratory, 2016. Document 810-005; http://deepspace.jpl.nasa.gov/dsndocs/810-005/.

[18] T. A. Ely and J. Seubert, "One-Way Radiometric Navigation with the Deep Space Atomic Clock," *Advances in the Astronautical Sciences*, Vol. 155, 2015, pp. 2799–2816.

[19] R. Lutwak, "The SA.45S Chip-Scale Atomic Clock," *2011 Stanford PNT Symposium*, Menlo Park, California, November 17–18, 2011.

[20] S. Asmar, "Ultra-Stable Oscillators for Probe Radio Science Investigations," *9th International Planetary Probe Workshop*, Toulouse, France, June 16–17, 2012.

[21] T.-H. You, A. Halsell, E. Graat, S. Demcak, D. Highsmith, S. Long, R. Bhat, N. Mottinger, E. Higa, and M. Jah, "Navigating Mars Reconnaissance Orbiter: Launch Through Primary Science Orbit," *AIAA SPACE 2007 Conference & Exposition*, Long Beach, California, September 18-20, 2007. AIAA Paper 2007-6093.

APPENDIX - TABULATED DATA

NOTE: All covariance values presented in this analysis are 1-σ unless otherwise noted. The approximate values presented here represent a specific analysis case for Earth-trailing / inner solar system applications and should ONLY be used to estimate orders of magnitude. As always, the best course of action is to conduct your own analysis for your specific use case. All one-way measurement type results tabulated here assume the use of a Chip-Scale Atomic Clock[19] that is currently being evaluated for future use on SmallSats; currently available clocks suitable for SmallSat applications are much less precise.

Table 5. Two-way Doppler-only position reconstruction accuracy at data cut-off. Approximate values of the principal axes of the uncertainty ellipsoid, in km.

Passes	**Pass Duration**				
Per Week	30 min.	1 hr.	2 hrs.	4 hrs.	8 hrs.
1	(406.8, 58.26, 31.48)	(237.49, 35.27, 30.85)	(138.26, 31.77, 19.99)	(46.57, 31.46, 9.87)	(31.73, 14.68, 3.24)
2	(251.17, 31.82, 18.92)	(94.79, 31.79, 18.52)	(42.6, 31.64, 16.26)	(31.15, 21.45, 6.81)	(28.85, 10.26, 2.06)
3	(196.26, 31.69, 16.66)	(79.94, 31.64, 16.29)	(36.88, 31.23, 14.23)	(30.58, 18.11, 5.54)	(26.55, 9.03, 1.77)
7	(105.59, 30.89, 12.42)	(55.39, 30.61, 10.88)	(30.46, 27.72, 8.02)	(28.79, 13.2, 3.24)	(21.34, 5.47, 1.25)

Table 6. Two-way Doppler-only velocity reconstruction accuracy at data cut-off. Approximate values of the principal axes of the uncertainty ellipsoid, in mm/sec.

Passes	**Pass Duration**				
Per Week	30 min.	1 hr.	2 hrs.	4 hrs.	8 hrs.
1	(87.11, 25.67, 7.09)	(56.37, 17.74, 6.21)	(37.49, 11.22, 5.15)	(23.31, 7.42, 2.02)	(16.12, 6.07, 0.63)
2	(51.61, 12.85, 3.59)	(30.19, 12.29, 3.52)	(23.58, 9.92, 3.09)	(19.76, 6.95, 1.27)	(15.71, 5.81, 0.46)
3	(41.1, 6.26, 2.67)	(27.53, 6.24, 2.57)	(21.79, 6.04, 2.32)	(17.61, 5.43, 0.98)	(13.91, 4.68, 0.37)
7	(29.2, 5.82, 2.14)	(24.17, 5.65, 1.81)	(19.61, 5.45, 1.36)	(15.09, 5.05, 0.6)	(10.73, 3.79, 0.28)

Table 7. Two-way Doppler-only position prediction accuracy 6 weeks after data cut-off. Approximate values of the principal axes of the uncertainty ellipsoid, in km.

Passes	**Pass Duration**				
Per Week	30 min.	1 hr.	2 hrs.	4 hrs.	8 hrs.
1	(615.9, 202.2, 70.5)	(400.1, 130.5, 70.0)	(251.1, 94.6, 69.3)	(127.8, 82.2, 67.5)	(90.9, 79.3, 66.7)
2	(357.8, 80.1, 57.2)	(168.5, 78.2, 57.1)	(113.8, 71.0, 56.6)	(91.4, 64.3, 54.3)	(75.4, 61.9, 53.2)
3	(278.9, 62.6, 56.2)	(147.9, 62.6, 56.0)	(103.5, 62.4, 55.4)	(82.6, 62.0, 53.5)	(69.7, 59.9, 52.7)
7	(170.0, 61.6, 55.1)	(121.0, 61.6, 54.5)	(92.3, 61.5, 53.9)	(73.5, 60.9, 53.1)	(61.4, 58.2, 52.0)

Table 8. Two-way Doppler-only velocity prediction accuracy 6 weeks after data cut-off. Approximate values of the principal axes of the uncertainty ellipsoid, in mm/sec.

Passes Per Week	Pass Duration				
	30 min.	1 hr.	2 hrs.	4 hrs.	8 hrs.
1	(79.9, 29.2, 25.9)	(71.8, 29.0, 25.8)	(51.1, 28.7, 25.7)	(38.2, 28.4, 25.6)	(36.4, 27.3, 25.6)
2	(36.4, 29.1, 24.1)	(35.7, 28.8, 24.1)	(33.9, 28.0, 24.1)	(32.1, 27.2, 24.0)	(31.5, 26.3, 24.0)
3	(31.4, 28.9, 24.1)	(31.3, 28.6, 24.0)	(31.2, 27.8, 24.0)	(31.2, 26.8, 24.0)	(30.9, 25.9, 23.9)
7	(31.1, 28.7, 24.0)	(31.1, 28.2, 24.0)	(31.0, 27.3, 24.0)	(31.0, 26.2, 24.0)	(30.6, 25.1, 23.9)

Table 9. Two-way SRA-only position reconstruction accuracy at data cut-off. Approximate values of the principal axes of the uncertainty ellipsoid, in km.

Passes Per Week	Pass Duration				
	30 min.	1 hr.	2 hrs.	4 hrs.	8 hrs.
1	(313.46, 52.49, 0.0)	(233.01, 42.96, 0.0)	(209.12, 40.09, 0.0)	(122.32, 26.05, 0.0)	(44.36, 8.98, 0.0)
2	(145.54, 17.05, 0.01)	(67.54, 9.98, 0.01)	(36.04, 6.59, 0.0)	(26.55, 5.2, 0.0)	(19.18, 3.16, 0.0)
3	(121.91, 13.24, 0.0)	(51.29, 7.92, 0.0)	(24.08, 4.88, 0.0)	(15.69, 3.44, 0.0)	(12.04, 2.12, 0.0)
7	(12.03, 7.62, 0.0)	(9.09, 4.24, 0.0)	(7.0, 2.19, 0.0)	(4.3, 1.25, 0.0)	(2.3, 0.69, 0.0)

Table 10. Two-way SRA-only velocity reconstruction accuracy at data cut-off. Approximate values of the principal axes of the uncertainty ellipsoid, in mm/sec.

Passes Per Week	Pass Duration				
	30 min.	1 hr.	2 hrs.	4 hrs.	8 hrs.
1	(67.92, 21.92, 5.23)	(53.29, 17.63, 3.98)	(49.35, 16.42, 3.63)	(36.63, 12.13, 2.72)	(22.31, 4.69, 1.54)
2	(34.92, 10.84, 3.44)	(25.68, 7.93, 2.25)	(22.38, 5.52, 1.4)	(20.94, 4.46, 1.04)	(19.17, 3.64, 0.6)
3	(30.95, 3.38, 2.74)	(23.09, 2.66, 1.8)	(19.01, 2.02, 1.05)	(16.6, 1.8, 0.76)	(15.59, 1.7, 0.42)
7	(14.82, 2.14, 1.23)	(14.36, 1.47, 0.8)	(12.99, 1.37, 0.4)	(10.51, 1.32, 0.22)	(7.64, 1.28, 0.11)

Table 11. Two-way SRA-only position prediction accuracy 6 weeks after data cut-off. Approximate values of the principal axes of the uncertainty ellipsoid, in km.

Passes Per Week	Pass Duration				
	30 min.	1 hr.	2 hrs.	4 hrs.	8 hrs.
1	(467.3, 187.3, 63.6)	(356.4, 158.5, 63.1)	(326.2, 149.6, 63.1)	(230.7, 109.2, 63.0)	(124.6, 78.4, 62.8)
2	(219.4, 78.0, 50.1)	(131.5, 66.1, 49.8)	(103.2, 60.2, 49.6)	(95.7, 58.7, 49.6)	(88.7, 57.9, 49.5)
3	(187.7, 60.3, 49.8)	(112.2, 58.2, 49.7)	(86.5, 56.8, 49.6)	(77.5, 56.5, 49.5)	(74.5, 56.4, 49.5)
7	(70.8, 57.1, 49.7)	(69.5, 56.4, 49.5)	(65.9, 56.2, 49.5)	(60.4, 56.1, 49.5)	(56.3, 55.1, 49.5)

Table 12. Two-way SRA-only velocity prediction accuracy 6 weeks after data cut-off. Approximate values of the principal axes of the uncertainty ellipsoid, in mm/sec.

Passes Per Week	Pass Duration				
	30 min.	1 hr.	2 hrs.	4 hrs.	8 hrs.
1	(63.9, 29.1, 25.9)	(57.0, 29.0, 25.8)	(55.5, 29.0, 25.8)	(50.3, 28.8, 25.6)	(36.8, 28.0, 25.5)
2	(35.3, 28.9, 24.0)	(33.0, 28.5, 24.0)	(31.8, 28.0, 23.9)	(31.4, 27.5, 23.9)	(30.9, 27.0, 23.9)
3	(30.7, 28.8, 23.9)	(30.5, 28.3, 23.9)	(30.3, 27.4, 23.9)	(30.2, 26.7, 23.9)	(30.2, 26.3, 23.9)
7	(30.1, 26.3, 23.9)	(30.1, 26.1, 23.9)	(30.1, 25.7, 23.9)	(30.1, 25.1, 23.9)	(30.1, 24.5, 23.9)

Table 13. Two-way Doppler+SRA position reconstruction accuracy at data cut-off. Approximate values of the principal axes of the uncertainty ellipsoid, in km.

Passes Per Week	Pass Duration				
	30 min.	1 hr.	2 hrs.	4 hrs.	8 hrs.
1	(183.64, 37.74, 0.0)	(124.47, 26.88, 0.0)	(77.92, 14.39, 0.0)	(38.88, 7.78, 0.0)	(13.25, 3.14, 0.0)
2	(26.81, 5.64, 0.0)	(25.33, 5.1, 0.0)	(22.09, 3.8, 0.0)	(16.39, 2.8, 0.0)	(9.1, 1.89, 0.0)
3	(15.62, 3.59, 0.0)	(14.5, 3.26, 0.0)	(12.77, 2.53, 0.0)	(10.71, 1.9, 0.0)	(7.43, 1.48, 0.0)
7	(4.76, 1.3, 0.0)	(3.71, 1.03, 0.0)	(2.87, 0.8, 0.0)	(2.19, 0.63, 0.0)	(1.59, 0.51, 0.0)

Table 14. Two-way Doppler+SRA velocity reconstruction accuracy at data cut-off. Approximate values of the principal axes of the uncertainty ellipsoid, in mm/sec.

Passes Per Week	Pass Duration				
	30 min.	1 hr.	2 hrs.	4 hrs.	8 hrs.
1	(45.43, 15.65, 3.43)	(37.08, 12.52, 2.75)	(29.74, 7.88, 2.06)	(21.42, 4.12, 1.36)	(14.12, 2.09, 0.55)
2	(21.03, 4.49, 1.14)	(20.71, 4.35, 1.02)	(19.97, 4.07, 0.73)	(18.37, 3.45, 0.52)	(15.21, 2.76, 0.36)
3	(16.41, 1.8, 0.82)	(16.1, 1.77, 0.74)	(15.74, 1.74, 0.53)	(15.03, 1.69, 0.37)	(13.08, 1.58, 0.28)
7	(10.88, 1.32, 0.24)	(9.77, 1.31, 0.18)	(8.6, 1.29, 0.14)	(7.36, 1.27, 0.1)	(5.85, 1.23, 0.08)

Table 15. Two-way Doppler+SRA position prediction accuracy 6 weeks after data cut-off. Approximate values of the principal axes of the uncertainty ellipsoid, in km.

Passes Per Week	Pass Duration				
	30 min.	1 hr.	2 hrs.	4 hrs.	8 hrs.
1	(296.6, 141.8, 63.0)	(234.2, 111.2, 63.0)	(175.7, 86.1, 62.9)	(119.2, 77.1, 62.8)	(84.1, 74.9, 62.7)
2	(95.4, 58.7, 49.6)	(94.5, 58.6, 49.6)	(92.1, 58.3, 49.5)	(85.2, 57.7, 49.5)	(73.2, 57.1, 49.5)
3	(76.6, 56.6, 49.5)	(75.7, 56.5, 49.5)	(74.9, 56.4, 49.5)	(72.7, 56.4, 49.5)	(67.0, 56.3, 49.5)
7	(61.2, 56.1, 49.5)	(59.0, 56.1, 49.5)	(57.0, 56.0, 49.5)	(56.2, 54.8, 49.5)	(56.1, 52.9, 49.5)

Table 16. Two-way Doppler+SRA velocity prediction accuracy 6 weeks after data cut-off. Approximate values of the principal axes of the uncertainty ellipsoid, in mm/sec.

Passes Per Week	Pass Duration				
	30 min.	1 hr.	2 hrs.	4 hrs.	8 hrs.
1	(54.8, 29.0, 25.7)	(51.1, 28.8, 25.6)	(42.4, 28.4, 25.5)	(36.5, 27.9, 25.5)	(35.0, 26.9, 25.5)
2	(31.4, 27.6, 23.9)	(31.4, 27.5, 23.9)	(31.2, 27.2, 23.9)	(30.8, 26.8, 23.9)	(30.4, 26.2, 23.9)
3	(30.2, 26.6, 23.9)	(30.2, 26.5, 23.9)	(30.2, 26.4, 23.9)	(30.2, 26.2, 23.9)	(30.1, 25.7, 23.9)
7	(30.1, 25.2, 23.9)	(30.1, 24.9, 23.9)	(30.1, 24.7, 23.9)	(30.1, 24.5, 23.9)	(30.1, 24.2, 23.9)

Table 17. Two-way Doppler plus monthly DDOR position reconstruction accuracy at data cut-off. Approximate values of the principal axes of the uncertainty ellipsoid, in km.

Passes Per Week	Pass Duration				
	30 min.	1 hr.	2 hrs.	4 hrs.	8 hrs.
1	(78.51, 31.45, 14.75)	(53.96, 31.27, 11.94)	(39.77, 30.79, 6.48)	(33.38, 27.96, 3.41)	(30.65, 12.79, 2.24)
2	(41.36, 30.39, 2.94)	(39.26, 30.16, 2.9)	(33.04, 27.51, 2.65)	(29.57, 18.83, 2.13)	(25.3, 10.26, 1.57)
3	(41.0, 29.64, 2.86)	(38.11, 29.29, 2.8)	(31.58, 25.49, 2.48)	(27.57, 16.26, 1.93)	(22.35, 8.75, 1.42)
7	(40.31, 28.46, 2.88)	(35.67, 27.68, 2.73)	(29.46, 22.34, 2.25)	(23.81, 13.18, 1.59)	(16.94, 5.71, 1.1)

Table 18. Two-way Doppler plus monthly DDOR velocity reconstruction accuracy at data cut-off. Approximate values of the principal axes of the uncertainty ellipsoid, in mm/sec.

Passes Per Week	Pass Duration				
	30 min.	1 hr.	2 hrs.	4 hrs.	8 hrs.
1	(29.47, 21.67, 3.4)	(26.26, 16.61, 2.64)	(25.3, 10.31, 1.49)	(22.62, 7.07, 0.82)	(14.81, 6.06, 0.52)
2	(25.08, 5.46, 0.94)	(24.35, 5.45, 0.9)	(21.68, 5.37, 0.73)	(17.83, 5.07, 0.49)	(12.72, 4.44, 0.35)
3	(24.92, 5.29, 0.92)	(23.93, 5.27, 0.86)	(20.81, 5.16, 0.67)	(16.61, 4.69, 0.44)	(11.69, 3.92, 0.31)
7	(23.83, 5.18, 0.87)	(22.25, 5.12, 0.77)	(18.88, 4.9, 0.54)	(14.26, 4.12, 0.34)	(9.05, 3.03, 0.24)

Table 19. Two-way Doppler plus monthly DDOR position prediction accuracy 6 weeks after data cut-off. Approximate values of the principal axes of the uncertainty ellipsoid, in km.

Passes Per Week	Pass Duration				
	30 min.	1 hr.	2 hrs.	4 hrs.	8 hrs.
1	(166.8, 110.9, 56.8)	(127.5, 97.8, 56.5)	(117.1, 72.2, 55.3)	(104.3, 64.5, 53.7)	(73.4, 62.9, 53.2)
2	(116.0, 62.4, 53.3)	(112.4, 62.3, 53.3)	(99.6, 62.1, 53.2)	(83.5, 61.2, 52.9)	(66.8, 59.5, 52.5)
3	(115.2, 61.9, 53.2)	(110.3, 61.9, 53.2)	(95.7, 61.6, 53.1)	(79.0, 60.3, 52.8)	(64.0, 58.6, 52.1)
7	(110.7, 61.4, 53.1)	(103.0, 61.2, 53.1)	(87.9, 60.7, 52.9)	(71.2, 58.9, 52.3)	(57.9, 57.3, 51.3)

Table 20. Two-way Doppler plus monthly DDOR velocity prediction accuracy 6 weeks after data cut-off. Approximate values of the principal axes of the uncertainty ellipsoid, in mm/sec.

Passes Per Week	Pass Duration				
	30 min.	1 hr.	2 hrs.	4 hrs.	8 hrs.
1	(50.0, 28.9, 24.1)	(40.8, 28.8, 24.1)	(34.7, 28.4, 24.0)	(32.5, 27.8, 24.0)	(31.5, 26.1, 24.0)
2	(31.2, 28.7, 24.0)	(31.2, 28.6, 24.0)	(31.2, 27.9, 24.0)	(31.0, 26.9, 24.0)	(30.8, 25.6, 23.9)
3	(31.1, 28.7, 24.0)	(31.1, 28.5, 24.0)	(31.1, 27.7, 24.0)	(30.9, 26.6, 24.0)	(30.6, 25.3, 23.9)
7	(31.1, 28.4, 24.0)	(31.0, 28.0, 24.0)	(30.9, 27.2, 24.0)	(30.7, 26.0, 23.9)	(30.4, 24.8, 23.9)

Table 21. Two-way Doppler plus weekly DDOR position reconstruction accuracy at data cut-off. Approximate values of the principal axes of the uncertainty ellipsoid, in km.

Passes Per Week	Pass Duration				
	30 min.	1 hr.	2 hrs.	4 hrs.	8 hrs.
1	(31.32, 6.91, 0.56)	(31.22, 6.65, 0.55)	(30.53, 5.42, 0.5)	(27.99, 3.52, 0.41)	(24.32, 2.57, 0.36)
2	(17.78, 2.68, 0.32)	(17.71, 2.67, 0.32)	(17.6, 2.65, 0.32)	(17.19, 2.58, 0.31)	(15.96, 2.47, 0.3)
3	(16.42, 2.43, 0.3)	(16.37, 2.43, 0.3)	(16.33, 2.42, 0.3)	(16.14, 2.41, 0.3)	(15.12, 2.34, 0.3)
7	(14.93, 2.76, 0.4)	(14.87, 2.75, 0.4)	(14.78, 2.74, 0.4)	(14.41, 2.72, 0.4)	(12.79, 2.57, 0.39)

Table 22. Two-way Doppler plus weekly DDOR velocity reconstruction accuracy at data cut-off. Approximate values of the principal axes of the uncertainty ellipsoid, in mm/sec.

Passes Per Week	Pass Duration				
	30 min.	1 hr.	2 hrs.	4 hrs.	8 hrs.
1	(15.11, 9.11, 0.23)	(14.65, 8.99, 0.22)	(12.69, 8.21, 0.21)	(10.43, 6.21, 0.17)	(9.41, 4.96, 0.13)
2	(8.38, 3.26, 0.13)	(8.37, 3.25, 0.13)	(8.35, 3.22, 0.13)	(8.29, 3.12, 0.12)	(8.1, 2.9, 0.12)
3	(8.14, 2.94, 0.13)	(8.13, 2.93, 0.13)	(8.12, 2.92, 0.13)	(8.09, 2.89, 0.13)	(7.9, 2.74, 0.11)
7	(7.92, 2.66, 0.12)	(7.91, 2.65, 0.12)	(7.89, 2.63, 0.12)	(7.8, 2.58, 0.12)	(7.22, 2.37, 0.11)

Table 23. Two-way Doppler plus weekly DDOR position prediction accuracy 6 weeks after data cut-off. Approximate values of the principal axes of the uncertainty ellipsoid, in km.

Passes Per Week	Pass Duration				
	30 min.	1 hr.	2 hrs.	4 hrs.	8 hrs.
1	(78.7, 63.1, 53.6)	(77.2, 63.1, 53.6)	(70.7, 62.5, 53.3)	(63.4, 60.3, 52.6)	(61.0, 58.1, 52.0)
2	(58.3, 56.0, 51.1)	(58.3, 55.9, 51.1)	(58.3, 55.9, 51.1)	(58.1, 55.8, 51.0)	(57.8, 55.5, 50.9)
3	(57.9, 55.6, 50.9)	(57.9, 55.6, 50.9)	(57.9, 55.5, 50.9)	(57.8, 55.5, 50.9)	(57.5, 55.3, 50.7)
7	(57.5, 55.2, 50.7)	(57.5, 55.2, 50.7)	(57.5, 55.2, 50.7)	(57.4, 55.1, 50.6)	(57.0, 54.4, 50.4)

Table 24. Two-way Doppler plus weekly DDOR velocity prediction accuracy 6 weeks after data cut-off. Approximate values of the principal axes of the uncertainty ellipsoid, in mm/sec.

Passes Per Week	Pass Duration				
	30 min.	1 hr.	2 hrs.	4 hrs.	8 hrs.
1	(34.8, 25.7, 24.0)	(34.4, 25.6, 24.0)	(33.1, 25.4, 24.0)	(31.6, 25.1, 24.0)	(31.1, 24.9, 23.9)
2	(30.5, 24.6, 23.9)	(30.5, 24.6, 23.9)	(30.5, 24.6, 23.9)	(30.5, 24.6, 23.9)	(30.4, 24.6, 23.9)
3	(30.4, 24.6, 23.9)	(30.4, 24.6, 23.9)	(30.4, 24.6, 23.9)	(30.4, 24.6, 23.9)	(30.4, 24.6, 23.9)
7	(30.3, 24.6, 23.9)	(30.3, 24.6, 23.9)	(30.3, 24.6, 23.9)	(30.3, 24.5, 23.9)	(30.3, 24.4, 23.9)

Table 25. One-way Doppler-only position reconstruction accuracy at data cut-off. Approximate values of the principal axes of the uncertainty ellipsoid, in km.

Passes Per Week	Pass Duration				
	30 min.	1 hr.	2 hrs.	4 hrs.	8 hrs.
1	(2868.98, 69.36, 31.5)	(1100.65, 68.12, 31.5)	(438.68, 60.04, 31.48)	(216.04, 37.48, 31.12)	(75.92, 31.57, 17.42)
2	(1576.84, 31.82, 19.17)	(750.18, 31.81, 19.07)	(279.79, 31.81, 18.96)	(104.7, 31.76, 18.12)	(43.71, 31.38, 11.12)
3	(942.66, 31.78, 18.17)	(528.64, 31.76, 17.86)	(223.04, 31.73, 17.46)	(88.04, 31.62, 16.27)	(38.02, 30.93, 9.25)
7	(562.41, 31.69, 17.18)	(327.35, 31.61, 16.56)	(148.14, 31.5, 15.73)	(63.38, 31.15, 13.51)	(30.42, 28.32, 6.54)

Table 26. One-way Doppler-only velocity reconstruction accuracy at data cut-off. Approximate values of the principal axes of the uncertainty ellipsoid, in mm/sec.

Passes Per Week	Pass Duration				
	30 min.	1 hr.	2 hrs.	4 hrs.	8 hrs.
1	(581.96, 29.88, 7.41)	(224.54, 29.4, 7.37)	(93.09, 26.34, 7.14)	(51.71, 18.63, 6.17)	(27.38, 11.58, 3.38)
2	(281.04, 13.09, 3.67)	(135.67, 13.0, 3.64)	(56.05, 12.9, 3.61)	(31.3, 12.44, 3.43)	(23.79, 10.29, 2.13)
3	(158.2, 6.83, 3.07)	(91.11, 6.55, 2.95)	(44.79, 6.4, 2.83)	(28.36, 6.24, 2.61)	(22.03, 5.62, 1.62)
7	(93.12, 6.3, 2.81)	(57.77, 6.21, 2.69)	(34.23, 6.13, 2.52)	(25.22, 5.9, 2.19)	(19.81, 5.29, 1.17)

Table 27. One-way Doppler-only position prediction accuracy 6 weeks after data cut-off. Approximate values of the principal axes of the uncertainty ellipsoid, in km.

Passes Per Week	Pass Duration				
	30 min.	1 hr.	2 hrs.	4 hrs.	8 hrs.
1	(4143.9, 241.1, 70.6)	(1596.2, 236.9, 70.6)	(657.9, 208.6, 70.5)	(361.1, 138.3, 70.0)	(160.7, 96.0, 68.4)
2	(2133.3, 81.2, 57.3)	(1019.8, 80.8, 57.3)	(394.6, 80.3, 57.2)	(179.0, 78.6, 57.1)	(114.7, 71.6, 55.7)
3	(1239.7, 64.2, 56.5)	(700.8, 63.6, 56.4)	(311.9, 63.2, 56.3)	(156.0, 62.8, 55.9)	(104.8, 62.4, 54.1)
7	(733.1, 62.8, 56.3)	(435.1, 62.4, 56.1)	(218.6, 62.2, 55.9)	(129.0, 61.9, 55.2)	(93.0, 61.7, 53.5)

Table 28. One-way Doppler-only velocity prediction accuracy 6 weeks after data cut-off. Approximate values of the principal axes of the uncertainty ellipsoid, in mm/sec.

Passes Per Week	Pass Duration				
	30 min.	1 hr.	2 hrs.	4 hrs.	8 hrs.
1	(116.0, 35.4, 26.4)	(86.1, 30.8, 26.1)	(79.8, 29.3, 25.9)	(66.6, 29.0, 25.8)	(42.6, 28.7, 25.7)
2	(48.4, 30.2, 24.4)	(39.1, 29.6, 24.2)	(36.6, 29.1, 24.1)	(35.8, 28.8, 24.1)	(34.1, 28.1, 24.0)
3	(35.1, 29.3, 24.3)	(32.5, 29.1, 24.2)	(31.6, 28.9, 24.1)	(31.4, 28.6, 24.0)	(31.3, 27.8, 24.0)
7	(32.3, 29.1, 24.2)	(31.5, 29.0, 24.1)	(31.3, 28.8, 24.0)	(31.2, 28.4, 24.0)	(31.1, 27.4, 24.0)

Table 29. One-way SRA-only position reconstruction accuracy at data cut-off. Approximate values of the principal axes of the uncertainty ellipsoid, in km.

Passes Per Week	Pass Duration				
	30 min.	1 hr.	2 hrs.	4 hrs.	8 hrs.
1	(1116.28, 69.13, 0.0)	(450.33, 60.51, 0.0)	(262.64, 47.04, 0.0)	(214.78, 40.67, 0.0)	(123.27, 25.94, 0.0)
2	(574.67, 32.61, 0.02)	(236.71, 21.21, 0.02)	(104.47, 13.86, 0.01)	(52.46, 8.25, 0.01)	(31.9, 5.74, 0.0)
3	(412.79, 16.42, 0.0)	(198.21, 15.23, 0.0)	(84.55, 10.98, 0.0)	(38.03, 6.47, 0.0)	(20.43, 4.06, 0.0)
7	(19.74, 12.54, 0.0)	(16.49, 10.57, 0.0)	(12.45, 6.79, 0.0)	(9.91, 3.24, 0.0)	(7.11, 1.8, 0.0)

Table 30. One-way SRA-only velocity reconstruction accuracy at data cut-off. Approximate values of the principal axes of the uncertainty ellipsoid, in mm/sec.

Passes Per Week	Pass Duration				
	30 min.	1 hr.	2 hrs.	4 hrs.	8 hrs.
1	(227.3, 29.23, 6.94)	(94.19, 25.5, 6.1)	(58.57, 19.5, 4.54)	(50.36, 16.69, 3.72)	(36.27, 11.75, 2.78)
2	(104.78, 14.01, 5.86)	(48.19, 11.92, 4.13)	(29.75, 9.71, 2.95)	(24.18, 6.86, 1.85)	(21.84, 4.9, 1.18)
3	(73.36, 4.11, 3.09)	(40.84, 3.77, 2.97)	(26.72, 3.12, 2.41)	(21.47, 2.38, 1.43)	(18.16, 1.89, 0.86)
7	(17.41, 3.18, 1.32)	(16.42, 2.72, 1.29)	(15.46, 1.74, 1.14)	(14.23, 1.44, 0.61)	(12.35, 1.36, 0.34)

Table 31. One-way SRA-only position prediction accuracy 6 weeks after data cut-off. Approximate values of the principal axes of the uncertainty ellipsoid, in km.

Passes Per Week	Pass Duration				
	30 min.	1 hr.	2 hrs.	4 hrs.	8 hrs.
1	(1614.9, 240.3, 64.3)	(660.1, 212.6, 63.9)	(397.0, 170.7, 63.3)	(334.1, 151.1, 63.1)	(228.5, 108.6, 63.0)
2	(782.8, 105.4, 50.7)	(334.4, 84.7, 50.3)	(170.9, 72.8, 49.9)	(117.5, 63.0, 49.7)	(100.7, 59.4, 49.6)
3	(552.5, 61.5, 49.9)	(279.2, 61.0, 49.9)	(146.1, 59.5, 49.7)	(100.0, 57.5, 49.6)	(83.4, 56.6, 49.5)
7	(80.5, 58.4, 49.8)	(76.8, 57.8, 49.8)	(73.6, 56.7, 49.6)	(70.0, 56.3, 49.5)	(64.9, 56.2, 49.5)

Table 32. One-way SRA-only velocity prediction accuracy 6 weeks after data cut-off. Approximate values of the principal axes of the uncertainty ellipsoid, in mm/sec.

Passes Per Week	Pass Duration				
	30 min.	1 hr.	2 hrs.	4 hrs.	8 hrs.
1	(82.0, 31.0, 26.1)	(70.5, 29.3, 25.9)	(59.9, 29.1, 25.9)	(56.0, 29.0, 25.8)	(49.0, 28.8, 25.6)
2	(41.9, 29.4, 24.2)	(36.7, 29.0, 24.1)	(34.3, 28.8, 24.0)	(32.4, 28.4, 23.9)	(31.5, 27.8, 23.9)
3	(31.1, 29.3, 24.0)	(30.8, 28.9, 24.0)	(30.6, 28.6, 23.9)	(30.4, 28.0, 23.9)	(30.2, 27.1, 23.9)
7	(30.2, 26.9, 23.9)	(30.2, 26.6, 23.9)	(30.1, 26.4, 23.9)	(30.1, 26.0, 23.9)	(30.1, 25.5, 23.9)

Table 33. One-way Doppler+SRA position reconstruction accuracy at data cut-off. Approximate values of the principal axes of the uncertainty ellipsoid, in km.

Passes Per Week	Pass Duration				
	30 min.	1 hr.	2 hrs.	4 hrs.	8 hrs.
1	(231.53, 42.6, 0.0)	(221.35, 41.33, 0.0)	(191.7, 38.64, 0.0)	(130.3, 28.46, 0.0)	(64.84, 14.09, 0.0)
2	(64.77, 9.64, 0.01)	(51.23, 8.14, 0.01)	(41.05, 7.05, 0.0)	(33.0, 5.96, 0.0)	(25.9, 4.41, 0.0)
3	(48.99, 7.66, 0.0)	(37.18, 6.4, 0.0)	(28.52, 5.37, 0.0)	(21.89, 4.32, 0.0)	(16.71, 3.06, 0.0)
7	(15.39, 4.37, 0.0)	(12.49, 3.33, 0.0)	(10.23, 2.59, 0.0)	(8.27, 2.01, 0.0)	(6.31, 1.48, 0.0)

Table 34. One-way Doppler+SRA velocity reconstruction accuracy at data cut-off. Approximate values of the principal axes of the uncertainty ellipsoid, in mm/sec.

Passes Per Week	Pass Duration				
	30 min.	1 hr.	2 hrs.	4 hrs.	8 hrs.
1	(53.01, 17.6, 3.93)	(51.3, 17.05, 3.77)	(46.68, 16.02, 3.54)	(37.58, 12.82, 2.89)	(25.84, 7.09, 2.04)
2	(25.39, 7.8, 2.18)	(24.03, 6.86, 1.82)	(22.97, 6.02, 1.53)	(21.98, 5.2, 1.23)	(20.72, 4.31, 0.87)
3	(22.82, 2.66, 1.74)	(21.33, 2.38, 1.42)	(19.93, 2.15, 1.16)	(18.51, 1.95, 0.92)	(17.15, 1.8, 0.63)
7	(16.76, 1.51, 0.8)	(15.58, 1.45, 0.62)	(14.39, 1.41, 0.48)	(13.15, 1.37, 0.37)	(11.8, 1.33, 0.27)

Table 35. One-way Doppler+SRA position prediction accuracy 6 weeks after data cut-off. Approximate values of the principal axes of the uncertainty ellipsoid, in km.

Passes Per Week	Pass Duration				
	30 min.	1 hr.	2 hrs.	4 hrs.	8 hrs.
1	(354.3, 158.1, 63.1)	(341.2, 154.1, 63.1)	(306.1, 144.8, 63.1)	(238.3, 115.0, 63.0)	(148.9, 86.0, 62.9)
2	(128.7, 65.6, 49.8)	(116.2, 63.0, 49.7)	(107.6, 61.1, 49.7)	(101.5, 59.8, 49.6)	(95.8, 58.7, 49.5)
3	(110.0, 58.1, 49.7)	(99.0, 57.4, 49.6)	(91.0, 57.0, 49.6)	(84.8, 56.7, 49.5)	(80.0, 56.5, 49.5)
7	(78.1, 56.4, 49.5)	(74.0, 56.3, 49.5)	(70.4, 56.2, 49.5)	(67.0, 56.2, 49.5)	(63.5, 56.2, 49.5)

Table 36. One-way Doppler+SRA velocity prediction accuracy 6 weeks after data cut-off. Approximate values of the principal axes of the uncertainty ellipsoid, in mm/sec.

Passes Per Week	Pass Duration				
	30 min.	1 hr.	2 hrs.	4 hrs.	8 hrs.
1	(56.8, 29.0, 25.8)	(56.1, 29.0, 25.8)	(55.2, 29.0, 25.7)	(51.1, 28.9, 25.6)	(39.3, 28.4, 25.5)
2	(33.0, 28.5, 24.0)	(32.4, 28.4, 23.9)	(32.0, 28.1, 23.9)	(31.7, 27.8, 23.9)	(31.2, 27.4, 23.9)
3	(30.5, 28.3, 23.9)	(30.4, 28.0, 23.9)	(30.3, 27.6, 23.9)	(30.2, 27.2, 23.9)	(30.2, 26.8, 23.9)
7	(30.1, 26.7, 23.9)	(30.1, 26.4, 23.9)	(30.1, 26.1, 23.9)	(30.1, 25.7, 23.9)	(30.1, 25.4, 23.9)

Table 37. One-way Doppler plus monthly DDOR position reconstruction accuracy at data cut-off. Approximate values of the principal axes of the uncertainty ellipsoid, in km.

Passes Per Week	Pass Duration				
	30 min.	1 hr.	2 hrs.	4 hrs.	8 hrs.
1	(128.64, 114.8, 17.05)	(126.02, 106.52, 16.82)	(121.15, 80.55, 15.62)	(106.23, 63.54, 13.63)	(101.08, 58.39, 11.07)
2	(120.88, 116.87, 20.73)	(119.12, 100.92, 20.16)	(112.95, 70.23, 17.53)	(95.11, 55.99, 13.99)	(89.43, 49.48, 10.85)
3	(118.08, 103.19, 20.65)	(109.36, 90.5, 19.81)	(99.91, 62.78, 16.39)	(77.05, 50.57, 12.69)	(72.38, 42.76, 9.75)
7	(98.74, 63.19, 13.48)	(89.79, 61.17, 12.77)	(74.56, 53.12, 10.96)	(67.31, 38.26, 10.15)	(64.3, 23.68, 7.89)

Table 38. One-way Doppler plus monthly DDOR velocity reconstruction accuracy at data cut-off. Approximate values of the principal axes of the uncertainty ellipsoid, in mm/sec.

Passes Per Week	Pass Duration				
	30 min.	1 hr.	2 hrs.	4 hrs.	8 hrs.
1	(39.09, 33.58, 23.47)	(38.2, 32.04, 23.15)	(36.47, 28.05, 20.96)	(33.52, 26.45, 17.18)	(32.36, 24.56, 15.22)
2	(38.43, 31.2, 23.47)	(36.47, 29.39, 22.82)	(33.7, 26.5, 19.24)	(30.27, 25.54, 15.29)	(29.1, 22.42, 13.05)
3	(37.89, 29.6, 23.4)	(34.91, 27.95, 22.39)	(31.34, 25.98, 17.92)	(27.2, 24.94, 14.1)	(26.04, 21.04, 12.27)
7	(30.65, 24.34, 13.0)	(28.94, 24.04, 12.26)	(25.96, 22.97, 11.12)	(22.32, 21.77, 10.79)	(21.35, 17.18, 10.05)

Table 39. One-way Doppler plus monthly DDOR position prediction accuracy 6 weeks after data cut-off. Approximate values of the principal axes of the uncertainty ellipsoid, in km.

Passes Per Week	Pass Duration				
	30 min.	1 hr.	2 hrs.	4 hrs.	8 hrs.
1	(236.8, 207.9, 115.6)	(226.8, 198.4, 115.1)	(214.1, 157.5, 111.3)	(194.1, 132.9, 99.5)	(186.9, 125.4, 88.4)
2	(233.5, 190.7, 115.3)	(215.6, 177.6, 114.2)	(196.5, 138.0, 106.1)	(172.5, 124.1, 89.2)	(165.0, 111.8, 78.6)
3	(230.7, 173.9, 115.0)	(205.2, 161.2, 113.4)	(179.5, 129.7, 101.1)	(149.3, 119.7, 84.2)	(142.9, 103.7, 76.0)
7	(180.0, 124.2, 81.2)	(166.5, 123.0, 78.3)	(141.6, 118.7, 73.2)	(128.1, 103.3, 71.7)	(123.6, 82.6, 68.1)

Table 40. One-way Doppler plus monthly DDOR velocity prediction accuracy 6 weeks after data cut-off. Approximate values of the principal axes of the uncertainty ellipsoid, in mm/sec.

Passes Per Week	Pass Duration				
	30 min.	1 hr.	2 hrs.	4 hrs.	8 hrs.
1	(61.1, 30.2, 28.9)	(57.9, 30.2, 28.9)	(49.8, 29.9, 28.9)	(44.5, 29.3, 28.7)	(43.1, 28.8, 28.1)
2	(60.3, 30.0, 28.9)	(55.0, 29.9, 28.9)	(46.0, 29.6, 28.8)	(41.2, 29.0, 28.6)	(39.7, 28.4, 27.8)
3	(59.6, 29.9, 28.9)	(53.0, 29.8, 28.9)	(43.7, 29.3, 28.8)	(39.1, 28.8, 28.4)	(37.7, 28.3, 27.5)
7	(40.6, 29.0, 27.5)	(39.2, 28.9, 27.3)	(36.9, 28.8, 27.0)	(36.2, 28.0, 26.9)	(35.5, 26.7, 26.7)

Table 41. One-way Doppler plus weekly DDOR position reconstruction accuracy at data cut-off. Approximate values of the principal axes of the uncertainty ellipsoid, in km.

Passes Per Week	Pass Duration				
	30 min.	1 hr.	2 hrs.	4 hrs.	8 hrs.
1	(94.77, 7.16, 0.57)	(94.75, 7.14, 0.57)	(94.58, 7.04, 0.56)	(88.39, 6.76, 0.55)	(88.12, 6.54, 0.53)
2	(92.26, 9.48, 0.76)	(92.19, 9.45, 0.76)	(91.74, 9.25, 0.75)	(82.68, 8.75, 0.72)	(81.93, 8.32, 0.67)
3	(83.85, 9.47, 0.76)	(83.75, 9.42, 0.76)	(83.11, 9.14, 0.75)	(69.12, 8.55, 0.71)	(68.14, 8.17, 0.67)
7	(67.06, 9.56, 1.29)	(66.74, 9.29, 1.24)	(65.46, 8.9, 1.2)	(63.62, 8.74, 1.17)	(62.42, 8.48, 1.12)

Table 42. One-way Doppler plus weekly DDOR velocity reconstruction accuracy at data cut-off. Approximate values of the principal axes of the uncertainty ellipsoid, in mm/sec.

Passes Per Week	Pass Duration				
	30 min.	1 hr.	2 hrs.	4 hrs.	8 hrs.
1	(31.52, 15.91, 11.01)	(31.51, 15.87, 11.0)	(31.44, 15.63, 10.96)	(30.18, 14.91, 10.66)	(30.07, 14.46, 10.43)
2	(30.1, 15.85, 10.99)	(30.08, 15.79, 10.98)	(29.94, 15.45, 10.91)	(28.24, 14.53, 10.43)	(28.03, 13.86, 9.98)
3	(28.53, 15.72, 10.76)	(28.51, 15.63, 10.74)	(28.29, 15.17, 10.64)	(25.79, 14.14, 9.85)	(25.47, 13.63, 9.43)
7	(22.61, 13.94, 9.29)	(22.47, 13.65, 9.14)	(22.08, 13.24, 8.91)	(21.53, 13.08, 8.76)	(21.05, 12.83, 8.57)

Table 43. One-way Doppler plus weekly DDOR position prediction accuracy 6 weeks after data cut-off. Approximate values of the principal axes of the uncertainty ellipsoid, in km.

Passes Per Week	Pass Duration				
	30 min.	1 hr.	2 hrs.	4 hrs.	8 hrs.
1	(179.9, 78.0, 61.8)	(179.8, 77.9, 61.8)	(179.5, 77.1, 61.7)	(170.8, 75.0, 61.5)	(170.3, 73.5, 61.2)
2	(170.7, 77.8, 61.7)	(170.6, 77.6, 61.7)	(169.9, 76.6, 61.6)	(157.7, 73.9, 61.2)	(156.6, 71.6, 60.7)
3	(159.4, 77.7, 61.6)	(159.3, 77.4, 61.6)	(158.2, 76.0, 61.5)	(139.9, 72.9, 61.0)	(138.2, 71.1, 60.5)
7	(129.7, 72.2, 60.3)	(129.1, 71.2, 60.2)	(127.0, 69.8, 60.0)	(124.1, 69.3, 59.8)	(121.9, 68.4, 59.6)

Table 44. One-way Doppler plus weekly DDOR velocity prediction accuracy 6 weeks after data cut-off. Approximate values of the principal axes of the uncertainty ellipsoid, in mm/sec.

Passes Per Week	Pass Duration				
	30 min.	1 hr.	2 hrs.	4 hrs.	8 hrs.
1	(41.2, 28.8, 25.8)	(41.2, 28.8, 25.8)	(41.1, 28.8, 25.8)	(39.9, 28.5, 25.7)	(39.7, 28.4, 25.7)
2	(40.2, 28.8, 25.8)	(40.1, 28.7, 25.8)	(39.9, 28.6, 25.8)	(38.3, 28.4, 25.7)	(37.8, 28.2, 25.7)
3	(38.9, 28.7, 25.8)	(38.9, 28.7, 25.8)	(38.6, 28.6, 25.7)	(36.4, 28.3, 25.7)	(36.0, 28.1, 25.6)
7	(36.1, 26.9, 25.6)	(35.8, 26.9, 25.6)	(35.3, 26.9, 25.6)	(35.0, 26.8, 25.5)	(34.7, 26.7, 25.5)